Eur Biophys J (2007) 36:1049–1058
DOI 10.1007/s00249-007-0191-x

ORIGINAL PAPER

Follow-up of drug permeation through excised human skin with confocal Raman microspectroscopy

Ali Tfayli · Olivier Piot · Franck Pitre · Michel Manfait

Received: 12 February 2007 / Revised: 9 May 2007 / Accepted: 15 May 2007 / Published online: 13 June 2007

Abstract Skin is a multilayered organ which covers and protects the surface of human body by providing a barrier function against exogenous agents. Meanwhile, the efficacy of several topically applicated drugs is directly related to their penetration through the skin barrier. Several techniques are commonly used to evaluate the rate, the speed and the depth of penetration of these drugs, but few of them can provide real-time results. Therefore, the use of nondestructive and structurally informative techniques permits a real breakthrough in the investigations on skin penetration at a microscopic scale. Confocal Raman microspectroscopy is a nondestructive and rapid technique which allows information to be obtained from deep layers under the skin surface, giving the possibility of a real-time tracking of the drug in the skin layers. The specific Raman signature of the drug enables its identification in the skin. In this study, we try to follow the penetration of Metronidazole, a drug produced by Galderma as a therapeutic agent for Rosacea treatment, through the skin. The first step was the spectral characterization of Metronidazole in the skin. Then microaxial profiles were conducted to follow the penetration of the drug in the superficial layers, on excised human skin specimens. For more accurate information, transverse sections were cut from the skin and spectral images were conducted, giving information down to several millimeters deep. Moreover, the collected spectra permit us to follow the structural modifications, induced by the Metronidazole on the skin, by studying the changes in the spectral signature of the skin constituents.

Keywords Confocal Raman microspectroscopy · Drug penetration · Metronidazole · Skin

Presented at the joint biannual meeting of the SFB-GEIMM-GRIP, Anglet France, 14–19 October, 2006.

A. Tfayli · O. Piot · M. Manfait
MeDIAN Unit, CNRS UMR 6142, Faculty of Pharmacy,
University of Reims Champagne, Ardenne, France

F. Pitre
Department of Pharmaceutical Development,
Formulation laboratory, Galderma R & D,
Sophia, Antipolis, France

A. Tfayli (✉)
51 rue Cognacq Jay, 51096 Reims,
Champagne Ardenne, France
e-mail: ali.tfayli@univ-reims.fr

Introduction

Transdermal drug delivery systems have been increasingly used in the past 20 years, the cutaneous application of drugs offers obvious advantages such as: avoidance of the hepatic first-pass metabolic effect which is a serious consequence of oral administration, zero order absorption for local cure in case of skin pathologies, controlled drug release, non invasive drug delivery, and improved patient compliance (Barry 1987; Fujiwara et al. 2005; Song et al. 2005; Wagner et al. 2001).

The skin is a multilayered biomembrane with particular absorption characteristics. It is a dynamic, living tissue, and the process by which a drug is transported across the skin is a complex process. The absorption is influenced by many factors, e.g. physicochemical properties of the drug, vehicle, occlusion, concentration, exposure pattern, skin site on the body, etc. (EC 2002). Reproducible data and an exact knowledge of the local distribution of a drug topically applied to the skin are decisive prerequisites to understand

and optimize the mode of action of drugs, particularly in dermatopharmacokinetics (EC 2002; van de Sandt et al. 2004; Weigmann et al. 2005).

In this perspective, recent changes in European Union policy encourage the use of in vitro methods and the use of excised human skin has been adopted by the "Guideline test" 428 of the Organization for Economic Co-operation and Development (OECD) (OECD 2004a). This approach offers the possibility to perform several replicate measurements from the same or a number of different subjects, and avoids ethical problems.

In fact, several techniques are used for evaluating drug delivery and diffusion into the skin and skin structures. A wide-spread method is diffusion cells, in which, the excised skin is mounted on the cell, and the drug preparation is applied to the surface of the skin. The underside of the skin is in contact with a receptor fluid. The diffusion of the drug through the skin is evaluated by measuring its concentration in the receptor fluid after a given time of diffusion (generally several hours) (Khan et al. 2005; van de Sandt et al. 2004; Wagner et al. 2001). This method lacks accuracy and cannot be used for drugs whose penetration is limited to the outermost layers (stratum corneum) of the skin.

Another widely used technique is "tape-stripping" which consists of removing the stratum corneum step-by-step with an adhesive tape (Kalia et al. 1998; Rawlings et al. 1994; Weigmann et al. 2005). This method is destructive and lacks spatial resolution.

Recently, biophysical techniques like Electron Microscopy (EM) (Hofland et al. 1995), Small Angle X-ray Scattering technique (SAXS) (Bouwstra et al. 1991), Confocal Laser Scanning Microscopy (CLSM) (Grams et al. 2004a, b; Veiro and Cummins 1994), and Two Photon Microscopy (TPFM) (Yu et al. 2003), have provided invaluable information about the speed and depth of penetration and the interaction of exogenous molecules and substances with the skin. The advantage of these methods is the high resolution that can be achieved; however, they do not provide molecular nor structural information.

Vibrational spectroscopy presents the advantage of providing molecular information directly from the skin. Infrared spectroscopy (IR) has been used to study the stratum corneum hydration and permeability (Potts et al. 1985), and more recently, for tracking lipid permeation into skin (Mendelsohn et al. 2006; Xiao et al. 2005b).

Raman spectroscopy is a powerful laser spectroscopic technique that detects, like IR spectroscopy, the characteristic vibrational energy levels of a molecule. When light irradiates a molecule, most of the photons are scattered elastically. This elastically scattered light, which has the same frequency as the incident light, is termed Rayleigh scattering. A small amount of light, however, is scattered inelastically. The inelastically scattered light, termed Raman (Stokes and anti-Stokes) scattering, exhibits frequency shifts with respect to the incident light. These shifts correspond exactly to the vibrational energy transitions of the molecule. They can be analyzed by an optical dispersive system to be represented as spectra. The Raman spectrum can be considered as a spectral fingerprint of the molecule (Koningsten 1971).

The additional advantage of Raman spectroscopy compared to IR is its ability to provide confocal information presenting the possibility of in vivo analysis and, for example here, a real-time evaluation of drug permeation mechanisms.

Several works have used confocal Raman spectroscopy to study the skin and skin hydration by assessing water concentrations and the effects of moisturizing factors (Caspers et al. 2001, 2003; Chrit et al. 2005; Sieg et al. 2006). Temporal and spatial variations of the penetration-enhancer DMSO in the stratum corneum were also studied (Caspers et al. 2002). More recently, Xiao et al. (2004, 2005a, b) used the same technique for tracking phospholipids permeation into the skin.

In this work, we attempt to follow-up the penetration of Metronidazole, a drug produced by Galderma (http://www.galderma.com/; Galderma laboratories, Sophia Antipolis, France) as a therapeutic agent for Rosacea treatment. Rosacea is common but still misunderstood skin disorder affecting middle-aged and older adults. It is estimated to affect 45 million people worldwide. Often called "adult acne" but potentially far more serious. Rosacea primarily affects the skin of the face and typically first appears as a transient flushing or blushing on the nose, cheeks, chin or forehead, and is usually discovered at its early and mildest stages (Cohen et al. 2002).

Metronidazole is a molecule used for the treatment of Rosacea. Its mechanism of action is unclear, it is poorly absorbed after topical application and is shown to have an anti-inflammatory effect in Rosacea (Zip 2006).

In our study, the first step was to determine the spectral signature of Metronidazole in its solid and liquid form dissolved in a Transcutol solution. After the determination of spectral features which will be used to detect the Metronidazole–Transcutol solution, the drug solution was deposited on the skin surface and axial Z profiles were recorded to follow-up its penetration. The Z profiles consist of an in-depth scanning with a given increment through the skin. Afterwards, the skin was then frozen and cut into thin transverse slices in order to perform Raman imaging complementing the confocal experiments. In a final step, we investigated the effect of the Metronidazole on the skin molecular constituents by studying the spectral changes at the level of certain vibrations, specific for the lipid or protein content.

Materials and methods

Excised human skin

Full thickness human skin (Biopredic International, Rennes, France), obtained from plastic surgery around the abdomen, was used. The skin was stored at −80°C until the date of the study.

For confocal Raman analysis, a 1.5 × 1.5 cm^2 of skin were cut. The underside of the skin was plunged in a PBS medium (Invitrogen, UK) to maintain the hydration of the skin, and the epidermis was exposed to the air. Each spectral recording was 10 min long. Details about spectral acquisition are presented in the instrumentation paragraph.

Once the in-depth confocal measurement was performed, the skin was cryo-fixed and 20 µm transverse sections were cut by cryo-microtome, and deposited on CaF_2 slides. These slides are optimized for Raman spectroscopy, they do not give rise to any signal in the spectral region (620–1,810 cm^{-1}) of interest.

Spectral images were obtained using a 5 µm step in X and Y lateral directions. The acquisition protocol is detailed in the instrumentation section.

Metronidazole solution

The Metronidazole is a drug marketed by Galderma (http://www.galderma.com/; Galderma laboratories, Sophia Antipolis, France) for Rosacea treatment. It mainly acts against pathogenic cutaneous anaerobic bacteria suspected to be the cause of the disease. For our analysis, 18 µg of Metronidazole were dissolved in 1 ml of Transcutol (Diethylene Glycol Monoethyl). Spectra of pure Metronidazole in the solid state, Transcutol and Metronidazole dissolved in Transcutol (Gattefossé, France), were measured to identify the vibrational peaks of the molecule and the solvent.

To study the penetration of the solution through the excised human skin, 20 µl of the solution were deposited on the skin surface, the time of diffusion was 1 h for the first sample and 2 h for the second, for each test, we analyzed an untreated skin sample as a blank test. The same analysis was repeated four times. After the diffusion period, the skin surface was cleaned with a dry cotton swab, before that axial Z profiles were recorded. The Z profiles consist of an in-depth scanning through the skin. Raman spectra were collected at different focus points, from −10 µm (above the skin surface) to 40 µm (under the skin surface) with a 4 µm step.

Instrumentation, Raman spectrometer

Raman spectral acquisitions were performed with a Labram microspectrometer (Horiba Jobin Yvon, Lille France). The excitation source was a titanium sapphire laser (Spectra Physics) generating single mode laser light at 785 nm. Such a wavelength allows a good penetration of the light deeply into the skin, minimizes parasite fluorescence and does not cause any photochemical or thermal degradation. The power of the laser beam focalized on the sample was measured and maintained at 50 mW; which is non-destructive for biological samples.

The microspectrometer is equipped with an Olympus microscope and all measurements were recorded using a 100× objective (NA = 0.9). The nominal spot size at the sample was assessed to be 4 µm. To obtain Z profiles, the objective was mounted on a high precision piezoelectric focusing drive which allows vertical movements with a minimal step of 50 nm.

Light scattered by the tissue is collected through the same objective. Rayleigh elastic scattering is intercepted by a Notch filter which reduces its intensity by a 10^6 factor. A confocal pinhole rejects signals from out-of-focus regions in the sample. A multichannel CCD detector (Coupled Charge Device) (1,024 × 256 pixels) detects the Raman Stokes signal dispersed with a 4 cm^{-1} spectral resolution by a holographic grating (950 grooves/mm). The spectral range was from 620 to 1,810 cm^{-1}, the acquisition time of each spectrum was 2 times 10 s and the confocal pinhole was adjusted to 150 µm.

Spectral acquisition and pre-processing were performed using Labspec software (Horiba Jobin Yvon, Lille, France).

To reduce the influence of the instrument response in the spectra, firstly, we corrected the collected signal by subtracting the black current signal (the signal collected on the CCD detector with the laser switched off). Secondly, the detector response was corrected by dividing spectra by the black body (white light) signal. Finally, the CaF_2 and/or the optical system signals were subtracted.

All spectra were smoothed using a five points average smoothing, and baseline corrected using an automatic polynomial function. For spectral image treatment, the set of spectra were vector normalized on the whole spectral range.

Results

Spectral signature of Metronidazole

The first part of our study consisted of establishing spectral signatures specific for the Metronidazole and for the Metronidazole solution in the Transcutol (Fig. 1, Table 1). This enabled us to determine the most pertinent spectral features to detect the drug on the skin.

Given that the quantity of remaining drug on and/or in the skin was very small, it was evident that the signal for

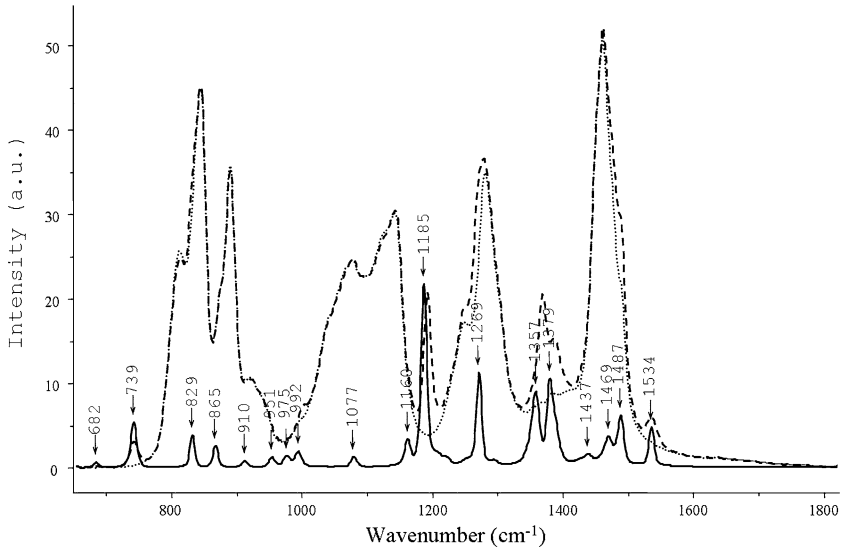

Fig. 1 Comparison between spectra of Metronidazole in its solid state (*solid line*), Metronidazole solution in Transcutol (*dashed line*), and Transcutol (*dotted line*). Three vibrational peaks (1,191 and 1,368 cm^{-1}) were selected to be used as Metrondazole markers in the skin

Table 1 Assignment of Metronidazole vibrations

Raman shift (cm^{-1})		
Metronidazole in solid state	Metronidazole solution	Assignment
681	684	
739	739	CH_2 rock (VPL[a])
829	Buried in the Transcutol signal	Ring breathing (Tsuboi et al. 1998)
865	Buried in the Transcutol signal	CH_3 rock, γ_t CH_2 (VPL[a])
910	Buried in the Transcutol signal	γ_w CH_2 (Parker 1983) CH_2 rocking (VPL[a])
951	Buried in the Transcutol signal	δ OH
972	Buried in the Transcutol signal	
992	Shoulder at 1,004	CH out of plane bend, ν ring (VPL[a])
1,077	Buried in the Transcutol signal	CH (Frost 2004)
1,160	Buried in the Transcutol signal	ν C–C (Schulte et al. 1995) CH (VPL[a]) ν CH_2 (Parker 1983)
1,185	1,191	559 + 646 (Frost 2004; Schulte et al. 1995) ν C–N (Parker 1983)
1,269	Buried in the Transcutol signal	N–O (VPL[a])
1,357	1,368	ν C–N (aromatic) (Parker 1983; VPL[a])
1,379	1,392	CH_2 scissor (Schulte et al. 1995) δ CH_3 (Sett et al. 2000)
1,436	Buried in the Transcutol signal	δ CH_3, CH_2 scissor, C–O (VPL[a])
1,469	Buried in the Transcutol signal	CO (Frost 2004) δ asym. CH_3 (Sett et al. 2000)
1,487	Shoulder	ν and δ of Ring (VPL[a]) CO (Frost 2004)
1,534	1,534	C=C

ν stretching, γ_w wagging, γ_t twisting, δ deformation

[a] VPL Molecular Spectroscopic Database, http://vpl.ipac.caltech.edu/spectra/allmolecules-list.htm

Metronidazole is very weak in intensity compared to the skin signal. Therefore, it was crucial to find some vibrations of the Metronidazole in spectral regions where the skin does not present any Raman signal. Figure 1 and the comparison with skin spectrum (data not shown) enabled us to select two vibration bands located at 1,191 and 1,368 cm^{-1} which can be used as markers for the drug.

Confocal Raman line maps

Although the acquisition time for each spectrum of confocal in depth profiles was limited to only 10 s, the quality of the obtained spectra is relatively good. Figure 2 shows a spectrum collected at a depth of 10 μm under the skin surface, spectral features arising from both the skin and the

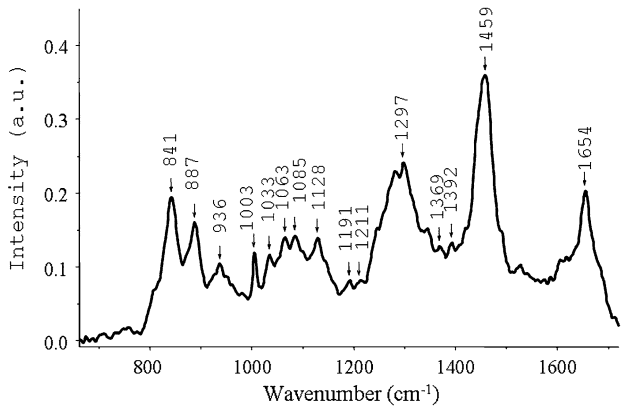

Fig. 2 Spectrum of Metronidazole solution in the skin

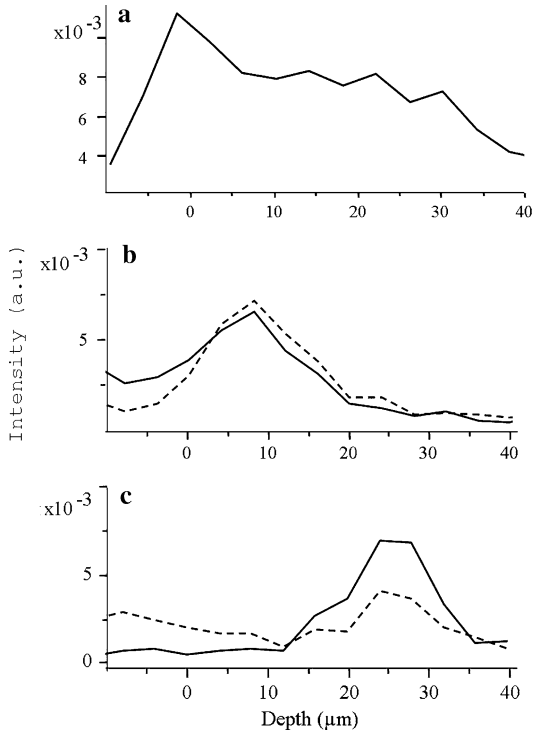

Fig. 3 **a** Confocal line map following the phenylalanine intensity variation through the skin. **b** Confocal line maps following the intensity of the bands at 1,191 cm^{-1} (*solid line*) and 1,369 cm^{-1} (*dashed line*), 1 h after topical application of the Metronidazole solution on the skin surface. **c** Confocal line maps following the intensity of the bands at 1,191 cm^{-1} (*solid line*) and 1,369 cm^{-1} (*dashed line*), 2 h after topical application of the Metronidazole solution on the skin surface

Metronidazole–Transcutol solution are clearly observed. For example, the 841 and 887 cm^{-1} bands correspond to the Metronidazole in Transcutol.

Endogenous lipids of the skin can be identified by the 936 and 1,297 cm^{-1} bands, corresponding respectively to the phospholipids and the ceramides. Spectral features arising from lipid conformation in the skin clearly appear at 1,063 cm^{-1} (hydrocarbon chain, *trans* conformation), and at 1,085 and 1,128 cm^{-1} (hydrocarbon chain, *gauche* conformation). The Raman CH deformation signal associated with lipids and proteins is present at 1,459 cm^{-1} (Parker 1983).

Protein content of the skin can be visualized by the Amide I and Amide III bands and several other weaker vibrations. Other features of current interest are the sharp phenylalanine-ring breathing vibration around 1,003 cm^{-1}, suitable for studying the protein content of the skin.

For this study, the most important features are the 1,191 and 1,369 cm^{-1} (ν C–N) stretching vibrations of the Metronidazole solution. The relative intensity of these bands, with respect of the skin protein bands intensities, indicates the relative concentration of Metronidazole, and the variation in their intensities reveals the deposition of the drug at different depths.

To evaluate the Metronidazole penetration, we needed to determine the exact position of the skin/air interface (depth = 0). For this, the zero position was determined by focusing the laser spot on the skin surface. Moreover, a Raman-based feature (phenylalanine of the skin at 1,003 cm^{-1}) was used to verify the skin/air interface position; the confocal line map, shown in Fig. 3a, follows the phenylalanine intensity profile from −10 µm to 40 µm. And it appears that the phenylalanine intensity increases from −10 µm to −2 µm and then starts to decrease progressively until 40 µm. Since the spectra are not normalised, the absolute intensity normally decreases with the depth and the higher intensity is obtained on the surface. This confirmed to us that the skin/air interface is precisely at −2 µm. The phenylalanine signal detected on the spectra from −10 to −2 µm (i.e. in the air) is due to the contribution of the skin surface.

The phenylalanine profile is compared with confocal line maps of the Metronidazole permeation, 1 h (Fig. 3b) and 2 h (Fig. 3c) after the topical application of the solution on the skin. This comparison gives semi-quantitative information about the drug deposition into the skin.

After 1 h diffusion, the Metronidazole is present under the skin surface and is detected down to 20 µm. One hour later, the Metronidazole is mainly detected between 14 and 34 µm.

The difference of the refractive index between the air and the skin, but also between the different skin layers, induce a deviation of the light beam; which gives a incorrect estimate of the depth value. This problem was studied and described by many groups (Baldwin and Batchelder 2001; Bruneel et al. 2002; Everall 2000a, b, 2004a, b) and a recent study by Xiao et al., using multilayered systems constituted with polymer films with refractive indexes close to those of the human skin, showed that the error in the measurement lead to an underestimation of the depth value of 15–20% (Xiao et al. 2004). Therefore, in the 1 h confocal

line map the Metronidazole is more likely to be present down to 23–24 μm rather than 20 μm. Similarly, in the 2 h confocal line map, it is more likely to be present between 15 and 40 μm rather than 14 and 34 μm.

Figure 4 shows a series of 14 Raman spectra of Metronidazole in the skin, measured with a 4 μm increment from −10 μm down to 40 μm under the surface (following the direction of the black arrow). These spectra were extracted from the 2 h line map. As the absolute intensity of spectra decreases with the depth, all spectra of this figure were vector normalized on the whole spectral range for a better visualisation. The spectra quality is still good even at depth, and different spectral features can still be identified. Several spectral variations can be distinguished, especially at 840 and 870 cm^{-1}, in the deeper spectra; these changes are due to the presence of Metronidazole–Transcutol solution. These bands mask the signal of the tyrosine Fermi doublet of the endogenous skin protein at 830–850 cm^{-1}; and the tryptophan vibration at 883 cm^{-1}. Other spectral differences can be seen at 1,191 and 1,369 cm^{-1} assigned to the stretching C–N vibrations of Metronidazole.

Figure 4 shows also the evolution of relative intensities of the 1,191 cm^{-1} band of the drug and of the 1,211 cm^{-1} band of the skin (phenylalanine, tryptophan and tyrosine). At the surface, the 1,211 cm^{-1} band is more intense than 1,191 cm^{-1} band. The deeper we progress into the skin, then the less intense is the 1,211 cm^{-1} feature and the higher is the intensity of the drug feature, especially between 16 and 40 μm (14–34 μm on the measuring scale).

Spectral imaging

To evaluate uncertainties in the confocal line map measurement induced by the difference in the refractive index between the air and the skin, skin samples were frozen and 20 μm thin slices were cut and deposited on CaF_2 slides. Spectral Raman images were then obtained. In Fig. 5, the image represents a section of skin 1 h after topical application of the Metronidazole solution. Figure 5b displays the variation of the integrated intensity of the 1,191 cm^{-1} Metronidazole vibration. A hair follicle is clearly seen, located perpendicular to the air/skin interface in this image. The reconstructed spectral image permits us to see that the Metronidazole is present down to 40–45 μm in the hair follicle, and to 25 μm for the stratum corneum. This is in agreement with the results obtained from confocal line map.

Effect of the Metronidazole–Transcutol solution on the skin

To inspect the effect of the Metronidazole–Transcutol solution on the skin structure, the spectra of in-depth profiles after 2 h of permeation were compared with spectra of the reference skin (untreated skin maintained for 2 h in similar conditions). In both cases the skin surface was cleaned with a dry cotton swab directly before the measurement.

In Fig. 6, spectra from superficial layers (stratum corneum) of both samples are presented. The absence of the 1,191 cm^{-1} feature indicates the absence of Metronidazole in the analyzed layers. Consequently, all spectral changes observed between the two specimens can be considered as a result of the effect of the drug on the skin constituents and not to the contribution of the drug in the skin signal.

No differences in the phenylalanine features are visible between the two models. This reveals that the protein content is similar in both samples. No variations were detected in the Amide I and Amide III bands which may lead us to conclude that there are no detectable changes in the protein secondary structure.

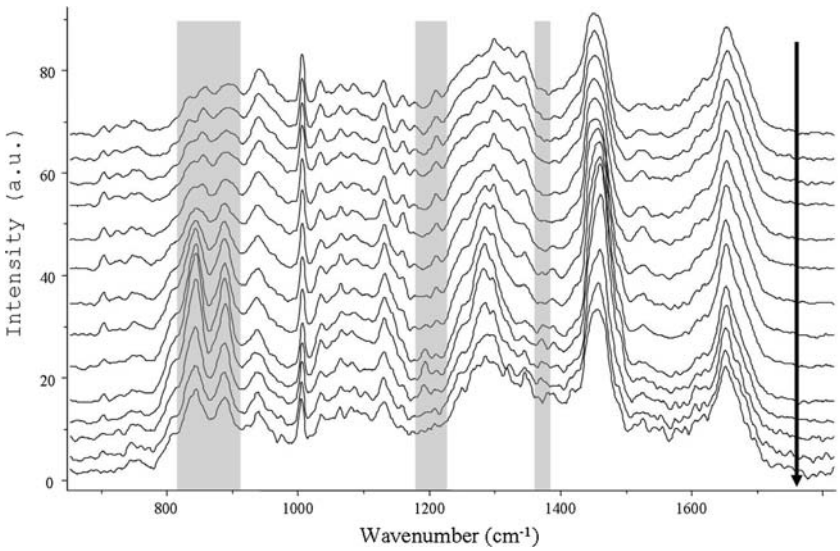

Fig. 4 Raman spectra from the 2 h line map showing the repartition of the Metronidazole in the skin

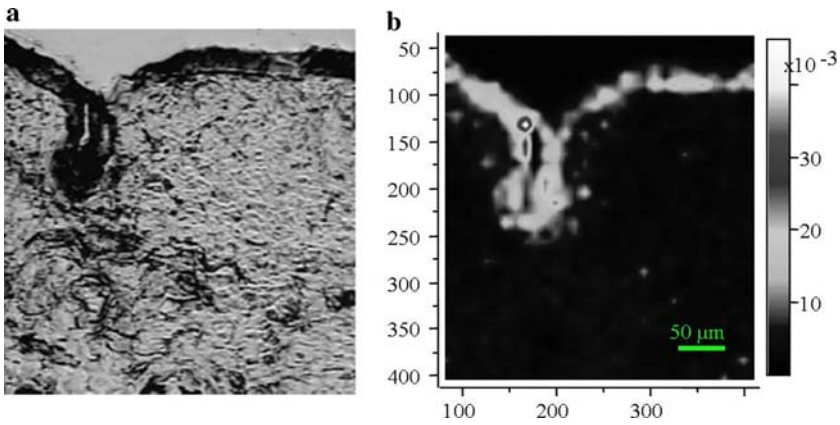

Fig. 5 **a** White light image. **b** Spectral image reconstructed on the integrated intensity of the 1,191 cm^{-1} feature

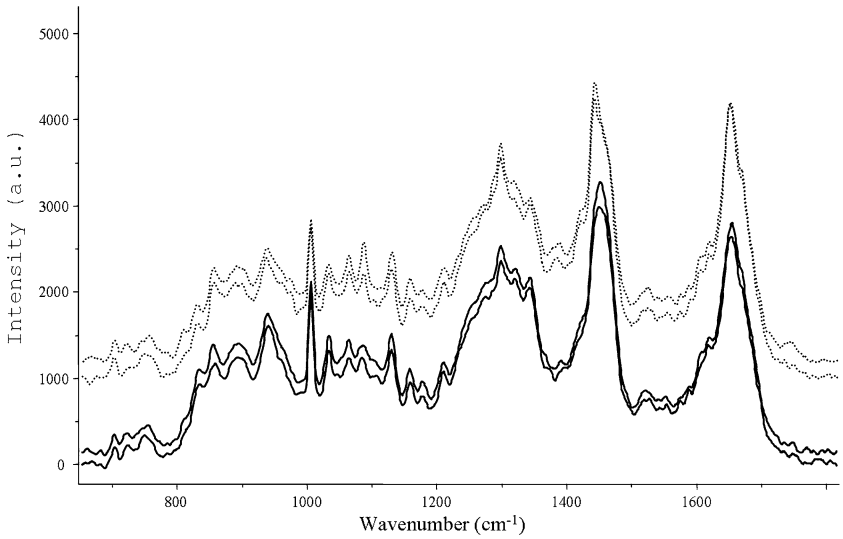

Fig. 6 Series of spectra from skin treated with Metronidazole solution (*solid lines*), and from untreated skin (*dotted lines*)

On the other hand, some changes are noted at 830 and 850 cm^{-1} vibrations. The 830/850 ratio of Fermi doublet of tyrosine is greater for the skin treated with the drug solution (Fig. 7a) than for the untreated sample. This doublet results from the Fermi resonance between the ring breathing vibration, and the overtone of the nonplanar ring vibration at 413 cm^{-1}. The intensity ratio I_{829}/I_{851} is related to the state of the phenolic hydroxyl group (Parker 1983). For both samples, the 851 cm^{-1} vibration is more intense which indicates that the phenolic OH group is an acceptor of hydrogen bonds; and that the tyrosyl residues are exposed and not "buried" within the protein. Such a configuration tends to form intermolecular bonds rather than intramolecular bonds.

The 883 cm^{-1} vibration is also more intense when skin is treated with Metronidazole–Transcutol solution (Fig. 7a). This feature is assigned to the tryptophan; it is shifted in frequency (from 873 to 883 cm^{-1}) when the residue is in aqueous liquid (Barry et al. 1992; Parker 1983; Piot 2000; Piot et al. 2000). The changes on the tyrosine and the tryptophan may be due to interactions between the solution and these residues.

Unlike the proteins, the endogenous lipid content and conformation are directly affected by the drug application. Figure 7a and b highlight the major changes induced by the Metronidazole–Transcutol solution. The 937 cm^{-1} vibration of lipids has a higher intensity on treated samples (Fig. 7a). Moreover, the CH deformation vibrations of lipids are clearly affected. This can be seen by the intensity of bands at 1,382 and 1,420 cm^{-1} (Fig. 6), these features remarkably are weaker for the treated skin. The frequency shift at the level of the maximum of the CH deformation band (around 1,450 cm^{-1}) confirms the involvement of the lipids. For the treated skin, the maximum is at 1,452 cm^{-1} whereas for untreated samples it is at 1,440 cm^{-1} (Fig. 7b).

The lipids present different conformations corresponding to different levels of organization. For example, the lipid fluidity increases with the decreasing number of the lateral bonds in the acyl chains, that is also associated with an increase of lipid disorganization (Gniadecka et al. 1998; Neubert et al. 1997; Wegener et al. 1997).

This fluidity and the intramolecular conformation can be studied by analysing the peak intensity in the 1,000–1,150 cm^{-1} region (Akhtar and Edwards 1997; Gniadecka

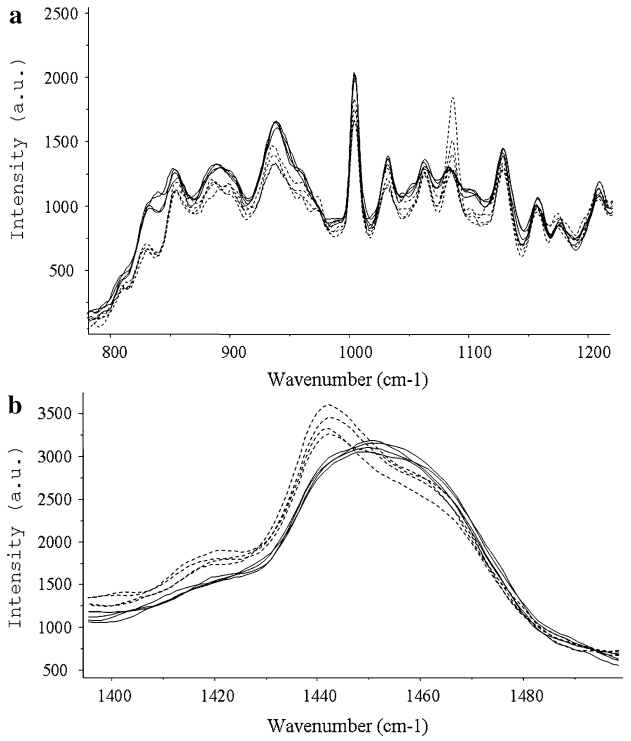

Fig. 7 Comparison between spectra of untreated skin (*dashed lines*) and treated skin (*solid lines*) in the 800–1,220 cm^{-1} region (**a**) and the 1,400–1,490 cm^{-1} region (**b**)

et al. 1998; Lippert and Peticolas 1971; Neubert et al. 1997; Wegener et al. 1997).

In the crystalline state, all the chains have a *trans* conformation, revealed by the presence of the 1,062 and 1,127 cm^{-1} peaks. The lipids disorganisation corresponds to a transition towards a *gauche* conformation, which is proved by the disappearance of the 1,062 and 1,127 cm^{-1} peaks simultaneously with the appearance of the 1,086 and 1,102 cm^{-1} peaks (Barry et al. 1992; Gniadecka et al. 1998; Neubert et al. 1997; Wegener et al. 1997).

In the both samples, the four features are present, but the treated skin presents weaker intensity for the 1,084 cm^{-1} feature (Fig. 7a), which indicates a decrease in the organized conformations of the lipid content of the skin.

Discussion

The possibility of tracking exogenous molecules in the skin has been demonstrated by previous works (Caspers et al. 2002; Xiao et al. 2005a, b). In their studies Xiao et al. used deuterated phospholipids. Labelling molecules with deuterium facilitates their detection, since C–D bonds arise between 2,000 and 2,250 cm^{-1}. A spectral domain free of vibrations from biological structures. The deuteration results in a chemical modification that is likely to affect some interaction mechanisms between the skin and the molecule. Therefore, in our study, we used a non-modified drug, solibulized in Transcutol, a common organic solvent employed by the pharmaceutical industry for drug formulation.

Since the drug and the solvent, both, present vibrations in the 600–1,800 cm^{-1} region, it was very important to determine the pertinent spectral features that could be used as signature for the Metronidazole solution.

The 1,191 and 1,369 cm^{-1} features were selected despite their relative weak intensity compared to other features of the drug solution. These two vibrations appear at wavenumbers where the skin does not present any Raman signal. These features enables us to detect the drug in the skin despite the very small concentrations employed for topical application.

Confocal line maps enabled: firstly, us to determine the position of the skin/air interface using Raman-based parameters. This was achieved by following the phenylalanine ring breathing at 1,003 cm^{-1}. Secondly, the Metronidazole penetration was determined by following the variation of the integrated intensity of the stretching C–N vibrations of the drug at 1,191 and 1,369 cm^{-1}. One hour after the application of the Metronidazole on the skin surface, it is detected at a depth of 23–24 μm and 1 h later it has been observed between 16 and 40 μm.

The uncertainties in the analysis depth, induced by the difference in the refractive index as described by previous works (Baldwin and Batchelder 2001; Bruneel et al. 2002; Everall 2000a, b, 2004a, b), were taken into account, and the measured value was considered to lead to an underestimation of the real depth by a factor of 15–20%. Therefore, the measured values were corrected by adding a 15–20% to each measurement. It is important to note that a high accuracy correction of the depth value is impossible. The estimated corrected value is considered as an approximation with a 2 μm margin of error.

The spectral imaging on the same samples, frozen directly after confocal measurements, enabled us to obtain more accurate values. The deposition of Metronidazole, after a 1 h period of permeation, was found in the stratum corneum, around 25 μm from surface; which confirms the results obtained from the confocal maps. The permeation was greater for the hair follicle.

The series of Raman spectra extracted from the 2 h line maps show that the signal of the Metronidazole–Transcutol solution is not detected at the level of the superficial layers. Therefore, the changes in the skin spectral features on these lines are due to the effect of the drug solution on the skin components. There is no contribution of the drug in the signal.

Several changes were detected due to the application of the Metronidazole–Transcutol solution on the skin, especially for

tyrosine and tryptophan vibrations. But the most important changes were observed on the lipid vibrations, such as the vibrations associated to C–H bonds at 1,392, 1,420 and 1,445 cm^{-1}, and the lipid feature at 937 cm^{-1}.

The lipid conformation was also affected, as revealed by a decrease in the intensity of the 1,084 cm^{-1} features (hydrocarbon chain: *gauche* conformation). This corresponds to a decrease in the organisation of the lipid content of the skin.

As a conclusion, using confocal Raman spectroscopy for such analysis presents multiple advantages. First, it enables the detection and the follow-up of exogenous molecules, or the determination of concentration profiles for endogenous molecules. Second, it enables information to be obtained about structures under the skin surface at a micrometric resolution. Third, there is no need for any special preparation. It is not destructive for the skin, and it can be used for in vivo measurements.

Finally, it gives direct structural information, and enables the changes in the skin to be monitored following the topical application of drug.

References

Akhtar W, Edwards HG (1997) Fourier-transform Raman spectroscopy of mammalian and avian keratotic biopolymers. Spectrochim Acta A Mol Biomol Spectrosc 53A:81–90

Baldwin KJ, Batchelder DN (2001) Confocal Raman microspectroscopy through a planar interface. Appl Spectrosc 55:517–524(8)

Barry BW (1987) Mode of action of penetration enhancers in human skin. J Controll Release 6:85–97

Barry BW, Edwards HGM, Williams AC (1992) Fourier transform Raman and infrared vibrational study of human skin: assignment of spectral bands. Raman Spectrosc 23:641–645

Bouwstra JA, de Vries MA, Gooris GS, Bras W, Brussee J, Ponec M (1991) Thermodynamic and structural aspects of the skin barrier. J Controll Release 15:209–219

Bruneel JL, Lassègues JC, Sourisseau C (2002) In-depth analyses by confocal Raman microspectrometry: experimental features and modeling of the refraction effects. J Raman Spectrosc 33:815–828

Caspers PJ, Lucassen GW, Carter EA, Bruining HA, Puppels GJ (2001) In vivo confocal Raman microspectroscopy of the skin: noninvasive determination of molecular concentration profiles. J Invest Dermatol 116:434–442

Caspers PJ, Williams AC, Carter EA, Edwards HG, Barry BW, Bruining HA, Puppels GJ (2002) Monitoring the penetration enhancer dimethyl sulfoxide in human stratum corneum in vivo by confocal Raman spectroscopy. Pharm Res 19:1577–1580

Caspers PJ, Lucassen GW, Puppels GJ (2003) Combined in vivo confocal Raman spectroscopy and confocal microscopy of human skin. Biophys J 85:572–580

Chrit L, Hadjur C, Morel S, Sockalingum G, Lebourdon G, Leroy F, Manfait M (2005) In vivo chemical investigation of human skin using a confocal Raman fiber optic microprobe. J Biomed Opt 10:44007

Cohen AF, Tiemstra JD (2002) Diagnosis and treatment of Rosacea. JABFP 15:214–217

EC (2002) Health consumer protection directorate, Directorate E, Guidance document on dermal absorption, vol Sanco/222/2000 rev.6. European commission

Everall NJ (2000a) Confocal Raman microscopy: why the depth resolution and spatial accuracy can be much worse than you think. J Appl Spectrosc 50

Everall NJ (2000b) Modeling and measuring the effect of refraction on the depth resolution of Confocal Raman Microscopy. J Appl Spectrosc 54

Everall NJ (2004a) Depth profiling with confocal Raman Microscopy, Part I. Spectroscopy 19. http://www.spectroscopyonline.com

Everall NJ (2004b) Depth profiling with confocal Raman Microscopy, Part II. Spectroscopy 19. http://www.spectroscopyonline.com

Frost RL (2004) Raman spectroscopy of natural oxalates. Anal Chim Acta 517:207–214

Fujiwara A, Hinokitani T, Goto K, Arai T (2005) Partial ablation of porcine stratum corneum by argon-fluoride excimer laser to enhance transdermal drug permeability. Lasers Med Sci 19:210–217

Gniadecka M, Faurskov Nielsen O, Christensen DH, Wulf HC (1998) Structure of water, proteins, and lipids in intact human skin, hair, and nail. J Invest Dermatol 110:393–398

Grams YY, Whitehead L, Cornwell P, Bouwstra JA (2004a) On-line visualization of dye diffusion in fresh unfixed human skin. Pharm Res 21:851–859

Grams YY, Whitehead L, Cornwell P, Bouwstra JA (2004b) Time and depth resolved visualisation of the diffusion of a lipophilic dye into the hair follicle of fresh unfixed human scalp skin. J Controll Release 98:367–378

Hofland HE, Bouwstra JA, Bodde HE, Spies F, Junginger HE (1995) Interactions between liposomes and human stratum corneum in vitro: freeze fracture electron microscopical visualization and small angle X-ray scattering studies. Br J Dermatol 132:853–866

Kalia YN, Pirot F, Potts RO, Guy RH (1998) Ion mobility across human stratum corneum in vivo. J Pharm Sci 87:1508–1511

Khan GM, Frum Y, Sarheed O, Eccleston GM, Meidan VM (2005) Assessment of drug permeability distributions in two different model skins. Int J Pharm 303:81–87

koningsten JA (1971) Introduction of the theory of the Raman effect. D. Reidel publishing

Lippert JL, Peticolas WL (1971) Laser Raman investigation of the effect of cholesterol on conformational changes in dipalmitoyl lecithin multilayers. Proc Natl Acad Sci USA 68:1572–1576

Mendelsohn R, Flach CR, Moore DJ (2006) Determination of molecular conformation and permeation in skin via IR spectroscopy, microscopy, and imaging. Biochim Biophys Acta 1758:923–933

Neubert R, Rettig W, Wartewig S, Wegener M, Wienhold A (1997) Structure of stratum corneum lipids characterized by FT-Raman spectroscopy and DSC. II. Mixtures of ceramides and saturated fatty acids. Chem Phys Lipids 89:3–14

OECD (2004a) Test guideline 428: skin absorption: in vitro method. Paris, France

Parker F (1983) Applications of infrared, Raman and Raman Resonance spectroscopy in biochemistry, New York

Piot O (2000) Caractérisation par microspectroscopie Raman des espèces moléculaires responsables de la cohésion des grains de blé tendre Pharmacy, vol Doctor. University of Reims Champagne - Ardenne, Reims

Piot O, Autran JC, Manfait M (2000) Spatial distribution of protein and phenolic constituents in wheat grain as probed by confocal Raman microspectroscopy. J Cereal Sci 32:57–71

Potts RO, Guzek DB, Harris RR, McKie JE (1985) A noninvasive, in vivo technique to quantitatively measure water concentration of the stratum corneum using attenuated total-reflectance infrared spectroscopy. Arch Dermatol Res 277:489–495

Rawlings AV, Scott IR, Harding CR, Bowser PA (1994) Stratum corneum moisturization at the molecular level. J Invest Dermatol 103:731–741

Schulte A, Bradley L, Williams C (1995) Equilibrium composition of retinal isomers in dark-adapted bacteriorhodopsin and effect of

high pressure probed by near-infrared Raman Spectroscopy. Appl Spectrosc 49:80–83

Sett P, Chattopadhyay S, Mallick PK (2000) Raman excitation profiles and excited state molecular configurations of three isomeric phenyl pyridines. Spectrochim Acta A Mol Biomol Spectrosc 56:855–875

Sieg A, Crowther J, Blenkiron P, Marcott C, Matts PJ (2006) Confocal Raman microspectroscopy—measuring the effects of topical moisturisers on stratum corneum water gradients in vivo. In: Mahadevan-Jansen A, Petrich WH (eds) The international society of optical engineering

Song Y, Xiao C, Mendelsohn R, Zheng T, Strekowski L, Michniak B (2005) Investigation of iminosulfuranes as novel transdermal penetration enhancers: enhancement activity and cytotoxicity. Pharm Res 22:1918–1925

Tsuboi M, Ezaki Y, Aida M, Suzuki M, Yimit A, Ushizawa K, Ueda T (1998) Raman scattering tensors of tyrosine. Biospectroscopy 4:61–71

van de Sandt JJM, van Burgsteden JA, Cage S, Carmichael PL, Dick I, Kenyon S, Korinth G, Larese F, Limasset JC, Maas WJM, Montomoli L, Nielsen JB, Payan JP, Robinson E, Sartorelli P, Schaller KH, Wilkinson SC, Williams FM (2004) In vitro predictions of skin absorption of caffeine, testosterone, and benzoic acid: a multicentre comparison study. Regul Toxicol Pharmacol 39:271–281

Veiro JA, Cummins PG (1994) Imaging of skin epidermis from various origins using confocal laser scanning microscopy. Clin Lab Invest 189:16–22

Wagner H, Kostka K-H, Lehr C-M, Schaefer UF (2001) Interrelation of permeation and penetration parameters obtained from in vitro experiments with human skin and skin equivalents. J Controll Release 75:283–295

Wegener M, Neubert R, Rettig W, Wartewig S (1997) Structure of stratum corneum lipids characterized by FT-Raman spectroscopy and DSC. III. Mixtures of ceramides and cholesterol. Chem Phys Lipids 88:73–82

Weigmann H-J, Jacobi U, Antoniou C, Tsikrikas GN, Wendel V, Rapp C, Gers-Barlag H, Sterry W, Lademann J (2005) Determination of penetration profiles of topically applied substances by means of tape stripping and optical spectroscopy: UV filter substance in sunscreens. J Biomed Opt 10:014009–014017

Xiao C, Flach CR, Marcott C, Mendelsohn R (2004) Uncertainties in depth determination and comparison of multivariate with univariate analysis in confocal Raman studies of a laminated polymer and skin. Appl Spectrosc 58:382–389

Xiao C, Moore DJ, Flach CR, Mendelsohn R (2005a) Permeation of dimyristoylphosphatidylcholine into skin—structural and spatial information from IR and Raman microscopic imaging. Vib Spectrosc 38:151–158

Xiao C, Moore DJ, Rerek ME, Flach CR, Mendelsohn R (2005b) Feasibility of tracking phospholipid permeation into skin using infrared and Raman microscopic imaging. J Invest Dermatol 124:622–632

Yu B, Kim KH, So PT, Blankschtein D, Langer R (2003) Visualization of oleic acid-induced transdermal diffusion pathways using two-photon fluorescence microscopy. J Invest Dermatol 120:448–455

Zip C (2006) An update on the role of topical metronidazole in rosacea. Skin Therapy Lett 11:1–4